FEBS Letters 566 (2004) 48–54 FEBS 28357

A tradeoff between protein stability and conformational mobility in homotrimeric dUTPases

Enikő Takács, Vince K. Grolmusz, Beáta G. Vértessy*

Institute of Enzymology, Hungarian Academy of Sciences, POB 7, H-1518, Budapest, Hungary

Received 3 February 2004; revised 3 April 2004; accepted 5 April 2004

Available online 28 April 2004

Edited by Peter Brzezinski

Abstract Oligomerization directs active site formation in homotrimeric 2′-deoxyuridine triphosphate pyrophosphatases (dUTPases). Stability of the homotrimer is a central determinant in enzyme function. The present comparative studies of bacterial and fruitfly dUTPases with homologous 3D structures by differential scanning microcalorimetry; fluorescence, circular dichorism and infrared spectroscopies, demonstrate that unfolding is a two-state highly cooperative transition in both dUTPases excluding a significantly populated intermediate state of dissociated and folded monomers. The eukaryotic protein is much less resistant against either thermal or guanidine hydrochloride-induced denaturation. Results suggest that hydrophobic packing of the inner threefold channel of the dUTPase homotrimer greatly contributes to stability.

Keywords: Stability; Oligomerization; Two-state unfolding; dUTPase; Microcalorimetry; Subunit interaction

1. Introduction

The 2′-deoxyuridine triphosphate pyrophosphatase (dUTPase) activity is indispensable to efficiently reduce cellular dUTP/dTTP ratios [1]. Elevated dUTP levels in lack of dUTPase result in erroneous incorporation of uracil into DNA. Uracil-subsituted DNA induces hyperactivity of base-excision repair and cell death due to DNA double strand breaks [2]. Most dUTPases are homotrimers with active sites at subunit interfaces (Fig. 2A) [3]. Oligomerization is therefore crucial to active site architecture in these enzymes.

Stability in oligomers is determined by the nature of intersubunit interactions. Such interactions in the dUTPase homotrimer fall into three classes (Fig. 2A) [4]. First, two neighbouring subunits create apolar contacts. Second, the C-terminal β-strand of the first subunit becomes integrated into the β-stranded jelly-roll fold of the second subunit. The C-terminal arm continues in crossing over the surface of the second subunit to reach the active site that receives conserved sequence motifs from the third subunit. Third, residues from all subunits contribute to form the central channel of the homotrimer. The three contact types were termed pairwise, arm-crossing and threefold interactions, respectively [5]. Pairwise and β-strand-swapping contacts are of highly similar character in all dUTPase homotrimers. However, threefold interactions within the central channel are greatly different. Hydropathy of these contacts was recently suggested to affect enzymatic mechanism in a way that linked increased polarity to cooperativity in substrate binding [6]. The major difference in threefold interactions may also significantly perturb stability of the homotrimer. In the prokaryotic enzyme, the inner channel is closely packed with apolar residues conserved among prokaryotic dUTPases. In human and Drosophila enzymes, only a small number of polar or charged residues are located in the channel at distances that preclude cohesive interactions except for a conserved Arg–Glu–Tyr H-bonded triad [5]. In addition to the conserved dUTPase sequence, the Drosophila enzyme also contains a flexible species-specific 28-residue C-terminal extension [6,7].

Here, we investigated stability of bacterial and Drosophila dUTPases, selected to represent pro- or eukaryotic homotrimers. Two types of denaturing forces (heat and chaotropic solvent) were applied and the unfolding process was followed by various independent experimental methods [differential scanning microcalorimetry (DSC), fluorimetry, circular dichroism (CD) and Fourier transform infrared (FT-IR) spectroscopy]. The homotrimer unfolds with no significant population of folded monomers. CD experiments demonstrate retention of some secondary structural elements after heat-induced unfolding. The bacterial enzyme, associated with packed apolar inner channel, presents considerably higher resistance against all denaturing conditions arguing that stability of the dUTPase homotrimer is mainly determined by the nature of the threefold interactions.

2. Materials and methods

Gel filtration materials were purchased from Amersham Biotech, USA, Phenol Red from Merck, Germany, dUDP from Jena Biosciences, Germany, and other chemicals from Sigma, US. α,β-Imino-dUTP was synthesized as in [6]. Enzymes were expressed and purified as previously [7,8]. Protein concentration was measured spectrophotometrically using $A^{0.1\%}_{1\,cm,\,280\,nm} = 0.32$, 0.26, or 0.52, for the Drosophila dUTPase constructs 1–159 (termed truncated), 1–187 (termed full-length), or bacterial dUTPase, respectively, [9]. Enzymatic activity was assayed by the continuous spectrophotometric method in 1 mM TES/HCl, pH 7.5, containing 40 μM dUTP, 5 mM MgCl2, 150 mM KCl, and 40 μM Phenol Red (assay buffer) ([7,10]).

* Corresponding author.
E-mail address: vertessy@enzim.hu (B.G. Vértessy).

Abbreviations: α,β-Imino-dUTP, 2′-deoxyuridine 5′-(α,β-imino)triphosphate; dUTPase, dUTP pyrophosphatase; DSC, differential scanning calorimetry; CD, circular dichroism; FT-IR, Fourier transformed infrared spectroscopy; GuHCl, guanidine hydrochloride

0014-5793/$22.00 © 2004 Federation of European Biochemical Societies. Published by Elsevier B.V. All rights reserved.
doi:10.1016/j.febslet.2004.04.039

2.1. CD measurements

Far UV CD spectra were recorded on a JASCO 720 spectropolarimeter in 1 mm pathlength thermostatted cuvette at 25 °C, using the protein samples at 0.2 mg/ml concentration in 20 mM Hepes buffer, pH 7.5, containing 5 mM $MgCl_2$ and 1 mM DTT (standard buffer). For denaturant-induced unfolding, guanidine hydrochloride (GuHCl) or urea was added to final concentrations from 0 to 8 M. For denaturation at high pH, the standard buffer was titrated by NaOH to reach pH 14. Heat-induced unfolding measurements were carried out in standard buffer also containing 10 mM KCl. Spectra were recorded at every second degree in the temperature range 20–80 °C. After reaching 80 °C, samples were cooled back to 20 °C.

2.2. FT-IR measurements

Infrared spectra were recorded on a Bruker IFS-28 FT-IR spectrometer, equipped with a DTGS detector. *Escherichia coli* dUTPase in 25 mM sodium phosphate buffer, pH 7.5, was lyophilized. Prior to the infrared experiments, the sample was dissolved in D_2O to a final concentration of 6 mg/ml and then measured between a pair of CaF_2 windows with 110 μm pathlength. Sample temperature was controlled by a thermostatted cell jacket. Spectra were obtained at 25, 35, 50, 60 and 70 °C (this latest value was the maximum allowed for the instrument). For each temperature, 128 scans were averaged. To decrease the water vapour lines, wet-air spectra were subtracted from the protein solution spectra in the wavenumber region of 1600–1700 cm^{-1}. The corrected spectra were deconvoluted using the built-in software of the Origin 5.0 package relying on Lorentzian curve fitting. During fitting, initial peak positions were based on second derivative spectra.

2.3. Analytical gel filtration

Protein samples in standard buffer also containing 3 M GuHCl were applied on Superdex 200HR column in a total volume of 100 μl, at a concentration of 5–10 mg/ml, with a flow rate of 0.5 ml/min. Alcohol dehydrogenase, ovalbumin, and lysozyme (150, 43, and 13.7 kDa, respectively) were used as molecular mass standards.

2.4. DSC

Calorimetric measurements were executed using the high sensitivity VP-DSC Microcalorimeter, following the manufacturer's instructions. Scans were recorded between 20 and 90 °C at 1 °C/min heating rate. Protein concentration was 0.2 mg/ml in 20 mM TES/HCl buffer, pH 7.5, containing 0.3 M NaCl, and 1 mM DTT. The melting temperature (T_m) was assigned to be the maximum of the excessive heat capacity function. Calorimetric enthalpies (ΔH_{cal}) were calculated from the area under the heat absorption curves [11]. Heat capacity functions were fitted to simple two-state transition model assuming the absence of experimentally observable intermediates. Fitted model curves were used to calculate van't Hoff enthalpies ($\Delta H_{van't\,Hoff}$) [11]. The effects of the nucleotide substrate ligands, tested at several different concentrations, were shown to level off at 5 mM dUMP, 250 μM dUDP or 100 μM α,β-imino-dUTP, respectively. These ligand concentrations were therefore assumed to be saturating and Mg^{2+} was used at 5 mM concentration in the experiments.

2.5. Fluorescence spectroscopy

Samples of bacterial dUTPase in standard buffer at 0.2 mg/ml concentration were measured using a JOBIN Fluoromax-3 spectrofluorimeter, in 1 ml thermostatted cuvettes. Tryptophyl emission spectra were recorded between 295 and 390 nm with excitation at 275–280 nm. For denaturant-induced unfolding, protein samples were incubated at varied denaturant concentrations ranging 0–6 M for 1 h on ice, and spectra were recorded at 25 °C. Reversibility of GuHCl-induced unfolding was checked by enzyme activity assays. Complete refolding performed by a 20-fold dilution of the protein unfolded in 4.5 M GuHCl into assay buffer at 15 °C took 40 min. Heat-induced change of fluorescence emission at 345 nm was recorded from 25 to 80 °C.

2.6. Data analyses

Raw data for heat-induced unfolding monitored by CD at 210 and 230 nm and by fluorescence emission at 345 nm were converted to the apparent fraction of native protein F_N, according to Eq. (1):

$$F_N = \frac{(\Theta_U + m_U T) - \Theta}{(\Theta_U + m_U T) - (\Theta_N + m_N T)} \quad (1)$$

where Θ is the observed spectroscopic signal at temperature T, Θ_N and Θ_U are the intercepts and m_N and m_U the slopes of the pre- and post-transitional base lines of the raw data, respectively. The F_N–T plot was then fitted to a two-state model using Eq. (2):

$$F_N = \frac{1}{1 + e^{\left[\Delta H(T/T_m - 1) + \Delta C_p(T_m - T - T\ln(T/T_m))\right]/RT}} \quad (2)$$

Initial estimates of T_m, ΔH_{cal} and the excessive heat capacity (ΔC_p) were from DSC experiments. The F_N–T plot was converted into the F_U–T plot by using the $F_N + F_U = 1$ equation, where F_U is the fraction of unfolded protein. Data from the excessive heat capacity function (DSC scans) were transformed into F_U–T plots by integration.

Raw data of GuHCl-induced equilibrium unfolding were fit to a two-state model using Eq. (3):

$$\Theta = \frac{\Theta_N + \Theta_U\left\{\exp\frac{m[D]-m[D]_{50\%}}{RT}\right\}}{1 + \left\{\exp\frac{m[D]-m[D]_{50\%}}{RT}\right\}} \quad (3)$$

where Θ is the observed spectroscopic signal measured at the actual concentration of the denaturant [D], Θ_N and Θ_U are the signals of the native and unfolded states, respectively, $[D]_{50\%}$ is the denaturant concentration at which the protein is 50% unfolded, m is the dependence of free energy on denaturant concentration (high m values indicating highly cooperative transitions), and T is the temperature at which the experiment was performed (25 °C).

3. Results and discussion

3.1. Two-state unfolding of dUTPases

Drosophila dUTPases 1–187 (full-length) and 1–159 (truncated, lacking the 28-residue fly-specific C-terminal extension) show T_m around 53 °C, while bacterial dUTPase melts at 74.5 °C (cf. [7], Fig. 1A). The significantly larger calorimetric enthalpy of the truncated 1–159 Drosophila dUTPase indicates that the 28-residue C-terminal extension may induce some destabilization of the folded protein, probably due to its high level of intrinsic disorder. To decide if binding of nucleotides or the Mg^{2+} co-factor induces any stabilizing effects on the protein, DSC scans were recorded in the presence of ligands. In previous experiments, saturating ligand concentrations were estimated from room-temperature dissociation constants [7]. In the present work, however, ligand saturation was tested experimentally anticipating heat-induced destabilization of protein–nucleotide complexes. In addition, the effect of the α,β-imino-dUTP, not probed previously, was also assessed.

Neither ligand induces any increment in T_m of bacterial dUTPase (Table 1). Nevertheless, binding of dUDP and, especially, that of α,β-imino-dUTP significantly increases ΔH_{cal} (Fig. 1B). In contrast, Mg^{2+}-binding to Drosophila dUTPases leads to a minor, but significant T_m increment, with gradual further increments in the presence of dUMP and α,β-imino-dUTP (Fig. 1C, Table 1). It is worthwhile to note that even the most stable Drosophila enzyme complex shows a much lower T_m than the bacterial protein. The dUDP inhibitor, previously shown to result in a dead-end enzyme complex [7,12], has smaller stabilizing effect on the fruitfly enzyme as compared to dUMP. This observation is in contrast with the previous finding where dUMP caused smaller effect [7]. The discrepancy is quite probably due to the increased concentration of the dUMP ligand in the present work, required for saturation during the melting process. The present data show that under saturating ligand concentrations, binding of the dUDP β-phosphate to dUTPase does not induce any further

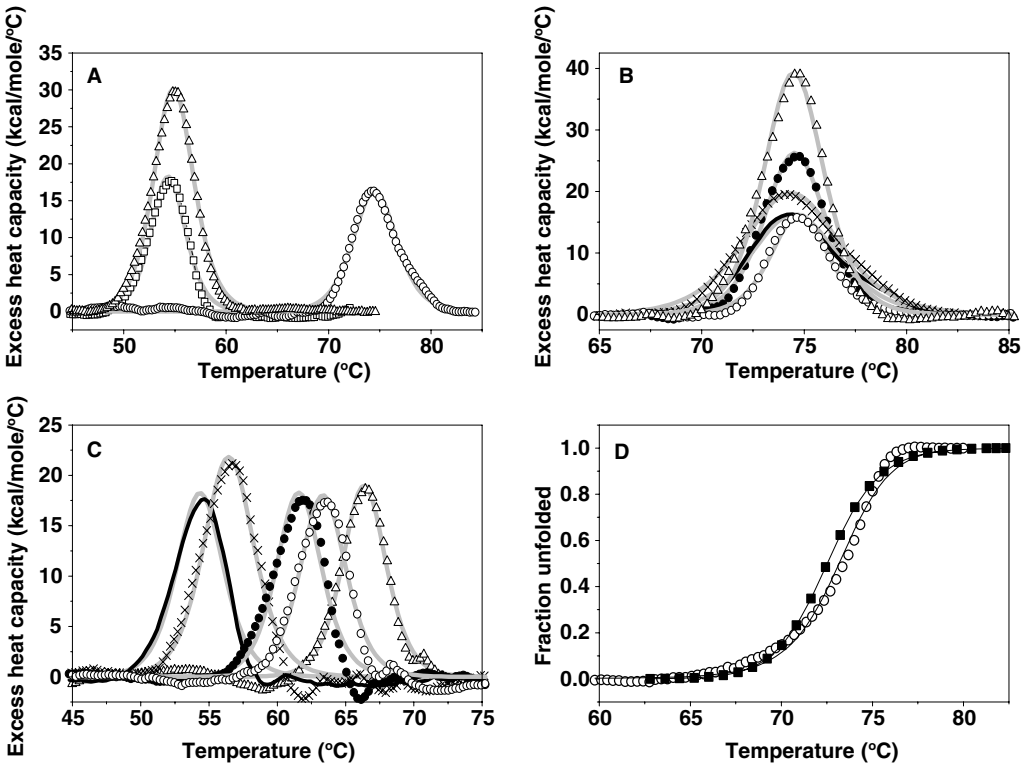

Fig. 1. Heat-induced unfolding of Drosophila and bacterial dUTPases. (A) Denaturation thermograms of Drosophila (1–159) dUTPase (△), Drosophila (1–187) dUTPase (□) and bacterial dUTPase (○), characterized with $\Delta H_{cal}/\Delta H_{van't\,Hoff}$ ratios of 0.97, 0.44, and 0.55, respectively. (B) and (C) Heat-induced denaturation of bacterial and Drosophila (1–187) dUTPase, respectively, without any ligand (solid line), in the presence of 5 mM $MgCl_2$ (crosses), with Mg^{2+} and 5 mM dUMP (◯), with Mg^{2+} and 250 μM dUDP (●), and with Mg^{2+} and 100 μM dUPNPP (△). $\Delta H_{cal}/\Delta H_{van't\,Hoff}$ ratios range from 0.40 to 0.90. (D) Comparison of thermal denaturation of bacterial dUTPase followed by partial heat capacity (■), as well as tryptophan fluorescence (◯), this latter measured at 280 nm excitation wavelength. Details of F_U–T plots are described in Experimental section. ΔH_{cal}, ΔC_p and T_m parameters for best fits were 92.8 kcal/mol, 0.85 kcal/mol/°C, 72.5 °C, and 92.8 kcal/mol, 0.85 kcal/mol/°C, and 73.1 °C, for the partial heat capacity and fluorimetric data, respectively.

Table 1
Melting temperatures of dUTPases, as determined in DSC experiments

Ligand added	*E. coli* dUTPase	Truncated *D. melanogaster* dUTPase	Full-length *D. melanogaster* dUTPase
None	74.5	54.9	54.4
Mg^{2+}	74.4	55.9	56.5
Mg^{2+} + dUMP	74.8	63.1	63.4
Mg^{2+} + dUDP	74.6	62.1	61.6
Mg^{2+} + α,β-imino-dUTP	74.5	64.6	66.4

Temperatures are given in °C.

stabilization of the enzyme, in agreement with previous limited trypsinolysis results [7].

To account for the ligand-induced conformational changes underlying the observed T_m increments, the ordering of the C-terminal conserved Motif 5, present in all dUTPases, should be considered. This ordering occurs in the same way in Drosophila dUTPase upon binding of either dUMP, dUDP or α,β-imino-dUTP [6], while it is induced only in the α,β-imino-dUTP–enzyme complex of bacterial dUTPase [13,14]. Therefore, the altered effects with the three nucleotides in the Drosophila system, and no T_m increasing effect in the bacterial system by any nucleotide cannot be fully explained by the C-terminal conformational shift on its own but suggest some additional structural change. Previous results in Drosophila enzyme–ligand complexes have, in fact, demonstrated that nucleotide binding results in increased resistance against proteolysis at multiple sites in the trimer [15].

DSC scans are indicative of protein oligomeric status during thermal unfolding. The present $\Delta H_{cal}/\Delta H_{van't\,Hoff}$ ratios are either close to unity or significantly lower (Fig. 1), arguing that homotrimers melt without dissociation into monomers and melting is accompanied with significant aggregation (cf. [7]). Partial reversibility of thermal unfolding was ascertained by multiple heating cycles, wherein heat capacity peaks were still observed (data not shown). To describe homotrimer melting with an independent technique, the single Trp residue of bacterial dUTPase was considered. The location of this residue within the inner threefold channel of the trimer [4] renders it a convenient endogenous probe to follow oligomerization status. Intrinsic Trp fluorescence is highly dependent on microenvironment [16], with an emission red-shift and a quantum yield decrease upon GuHCl-induced unfolding (cf. Fig. 5A, inset). Unfortunately, this technique is not applicable to fruitfly dUTPase lacking Trp residues. Fig. 1D depicts that changes in the unfolded protein fraction of bacterial dUTPase during heating display practically the same characteristics no matter which experimental technique is used. This close agreement indicates that translocation of the Trp residue of bacterial dUTPase from an apolar environment within the central channel to an aqueous solvent-exposed environment is concomitant with the unfolding transition associated with the

single heat-absorption peak of the DSC scan. Solvent-exposure of Trp may occur either due to dissociation of the homotrimer into folded monomers or due to complete unfolding. The first alternative would necessarily require a significant heat-absorption peak reflecting melting of these monomers after the fluorimetric transition. Lack of such peak strongly argues for two-state unfolding with no folded monomers.

The scheme of this unfolding pathway is shown in Fig. 2B. Results from fluorimetric and DSC experiments consonantly demonstrate that homotrimeric dUTPases unfold in a one-step transition. In this process, trimer dissociation and monomer unfolding occur in a concomitant way, not separable under the experimental conditions.

3.2. Distinct secondary structural elements with altered heat stability

In addition to the above techniques, CD spectroscopy may describe minor structural alterations, not necessarily involving large enthalpy changes. Both the character and the intensity of the CD spectrum of bacterial dUTPase are altered at high temperature (Fig. 3A). Interestingly, the spectrum recorded at high temperature develops a major shoulder in the 215–230 nm wavelength range that suggests some non-native structural ordering. This phenomenon is further discussed at the end of the present section. In agreement with the DSC data, CD spectra of heated dUTPase after recooling to room temperature reflected partial reversibility of thermal denaturation.

Interestingly, heating induced altered effects in different spectral regions. Depending on the wavelength where CD is measured, heating of the protein either increased or decreased ellipticity, with an isosbestic point at 218 nm (Fig. 3A and B). Wavelength-dependent transitions are characterized with different melting temperatures (Fig. 3C) to reflect distinct structural changes associated with altered enthalpies. The low resolution information content of the CD spectra unfortunately precluded direct assignment of CD transitions to distinct secondary structural elements. The assignment was further complicated by the rather unusual CD spectrum of the native dUTPase protein, which does not fully conform to the spectrum characteristic for a β-structured protein (Table 2, [10,17]). Based on the melting temperature values in comparison with the DSC data, we propose that CD changes in the lower wavelength regions (210 nm) may reflect local relaxation of some turns close to the protein surface, increasingly exposed to the solvent. These local effects do not require major enthalpy changes. The DSC heat absorption peak probably corresponds to the CD transition observed in the higher wavelength region (220–230 nm) reflecting the major unfolding process (Fig. 3C).

CD spectroscopy was also adequate for investigation of Drosophila dUTPase, where the absence of Trp residues prevented fluorimetric measurements. CD spectra recorded during thermal melting of the fruitfly enzyme (data not shown) possess very similar characteristics to the results obtained with the bacterial enzyme; the only difference being that the 220-nm-transition appears at a lower temperature in agreement with the DSC scans. It seems therefore that in both eu- and prokaryotic dUTPases (i) some conformational transitions occur with minor enthalpy changes, rendering them undetectable in DSC measurements, and (ii) some residual structure is maintained after thermal melting.

This residual structure was further investigated by performing thermal denaturation of the *E. coli* protein in the presence of a variety of chemical denaturing agents. The inset of Fig. 3D inset demonstrates that high concentration of either GuHCl or urea, as well as extreme high pH (pH 14) all induce significant unfolding, as reflected in perturbation of the CD spectrum. In the high temperature measurements, the additional unfolding effect of these denaturing agents is also evident (Fig. 3D main panel). However, for the two chaotropic agents used in these experiments, the unfolding effects are much more pronounced at ambient as compared to high temperature (compare CD changes induced by GuHCl at 25 and 80 °C, Fig. 3D inset and main panel, respectively). The decreased effect of these two agents is probably due to their reduced binding to the protein at high temperature [18,19]. The

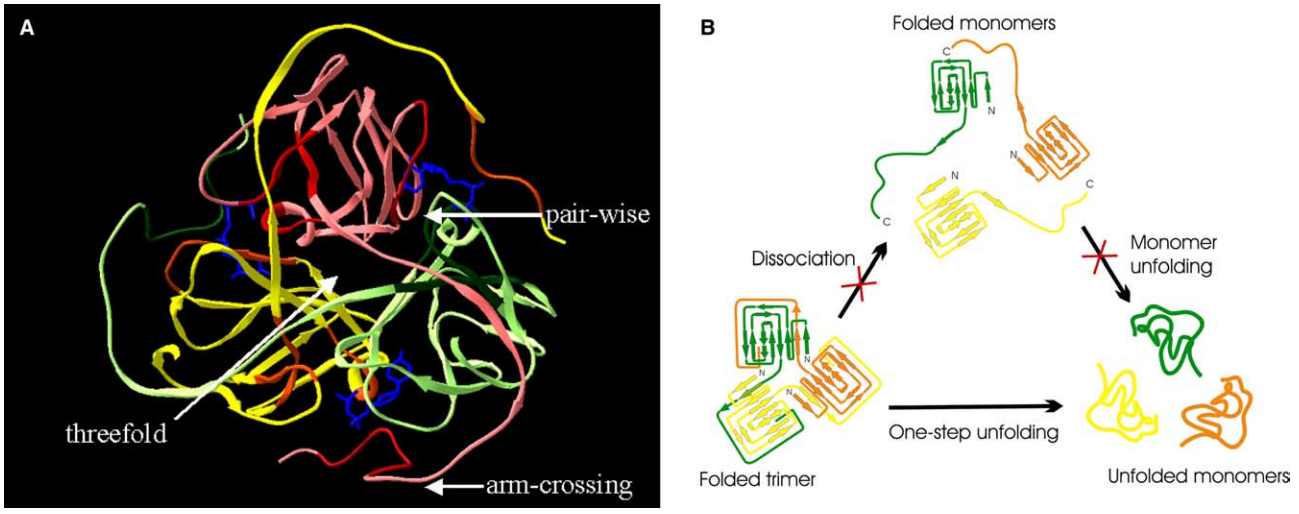

Fig. 2. Models of dUTPase structure and unfolding. (A) Monomer interactions in the dUTPase homotrimer (based on [21]). Arrows indicate the three types of interactions in ribbon representation of colour-coded oligomer, wherein the five conserved dUTPase motifs are depicted in dark shades. The dUDP ligands in the active sites are in blue colour. (B) Unfolding pathway in the dUTPase homotrimer. The model of the folded colour-coded oligomer (left) details the β-stranded jelly-roll fold.

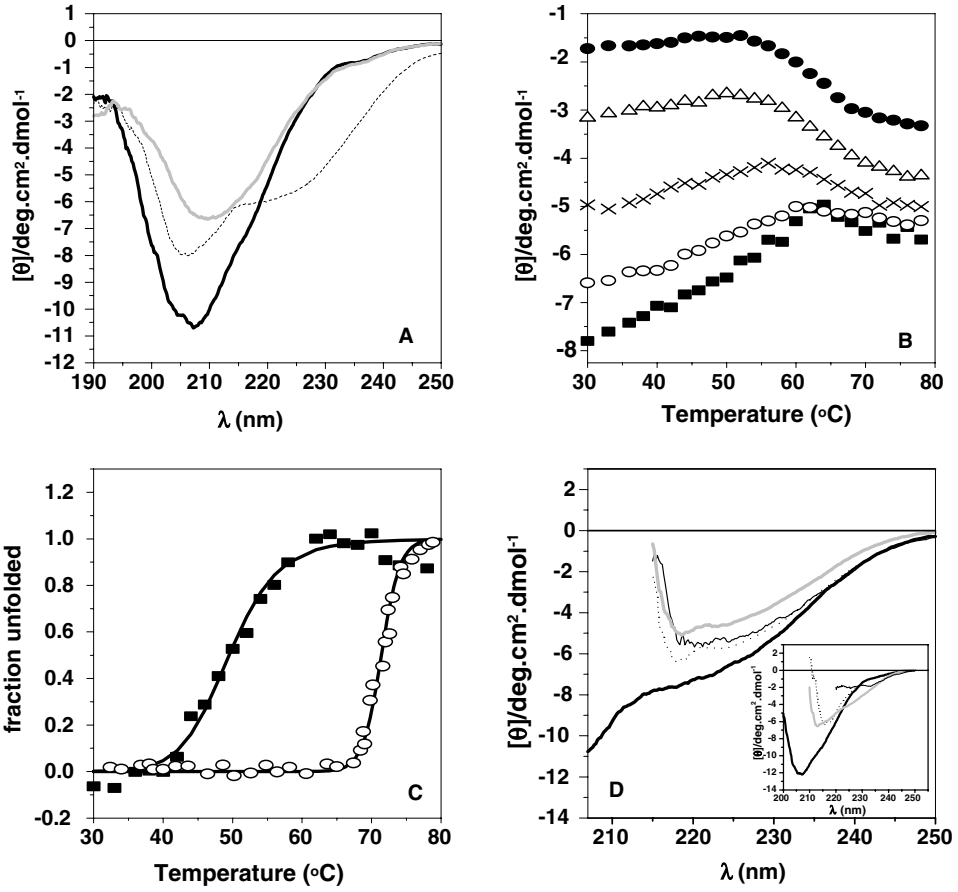

Fig. 3. Secondary structural elements during heat-induced unfolding. (A) CD spectra of bacterial dUTPase at 20 °C (solid black line), at 90 °C (dashed line), and cooled to 20 °C right after reaching 90 °C (solid grey line). (B) Temperature dependence of molar ellipticity of bacterial dUTPase at five different wavelengths, using the protein sample at 0.2 mg/ml concentration. From top to bottom: at 230 (●), 225 (△), 220 (crosses), 215 (○) and 210 (■) nm. (C) Apparent fraction of unfolded bacterial dUTPase monitored by ellipticity at 220 (○) and 210 (■) nm. The data sets were fitted to Eq. (2) (solid lines), with T_m values of 49.9 and 71.3 °C, respectively. (D, Main) CD spectra of *E. coli* dUTPase at 80 °C in the absence of denaturant (black thick line), 4.5 M GuHCl (black thin line), 8 M urea (dotted line) and at pH 14 (grey line). (D, Inset) CD spectra of *E. coli* dUTPase at 25 °C in the absence of denaturant (black thick line), 4.5 M GuHCl (black thin line), 8 M urea (dotted line) and at pH 14 (grey line).

Table 2
Estimation of secondary structural elements in *E. coli* dUTPase

Method	α-Helix (%)	β-Sheet (%)	Turn (%)	Other (%)
X-ray[a]	5	41	11	43
CD[b]	8	32	17	38
IR (35 °C)	17	48	14	21
IR (70 °C)	8	28	48	16

[a] Larsson et al. [4].
[b] Vertessy [10].

minor but significant spectral changes induced in the high temperature spectrum by chemical denaturants strengthen the assumption that these spectra reflect some residual secondary structure that can be perturbed by chaotropes or high pH.

An independent spectral technique was therefore used to provide more details on the protein structural elements at high temperature. Fig. 4 presents FT-IR spectra of *E. coli* dUTPase obtained at 35 and 70 °C in the wavenumber region characteristic for amide I′ band [20]. The high temperature spectrum shows an increased shoulder in the 1655–1690 cm^{-1} wavenumber interval. Within this region, amide I′ band reflects turn or extended chain peptide bond conformations [20]. Based on deconvoluted IR spectra, the relative amounts of secondary structural elements were assessed (Table 2.). Although it is evident that neither CD nor FT-IR can provide numerical data that are in perfect agreement with those calculated based on the high-resolution crystal structure, still, the temperature-induced changes are worthwhile to examine. At high temperature, the decrease in both α-helical and β-sheet conformations is accompanied by a significant increase in turn-like conformations. Results therefore suggest that high temperature may induce some non-native but still ordered conformations in *E. coli* dUTPase that shows FT-IR spectral characteristics reminescent of turn-like conformations. Measurements at considerably higher temperatures (80–90 °C), not accessible in our present experimental setup, would be required for further conclusive investigations of the non-native conformations in the *E. coli* protein.

3.3. Assessing protein stability with solvent-induced denaturation

Thermal unfolding studies demonstrated a major difference in stability of bacterial and Drosophila dUTPases. This conclusion should also be tested in solvent-induced denaturation experiments. As shown in the previous section, Trp fluorescence is a sensitive and adequate method to follow unfolding

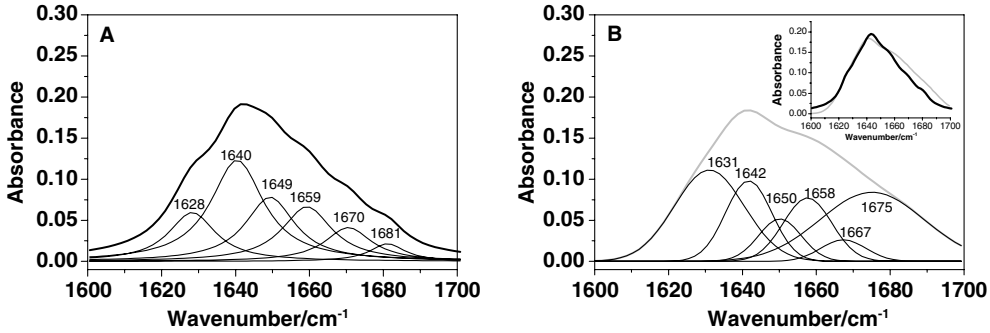

Fig. 4. FT-IR conformational analyses of *E. coli* dUTPase at 35 °C (A) and 70 °C (B). Infrared spectra of *E. coli* dUTPase at 35 °C (thick solid line) at 70 °C (thick grey line) are shown, together with the individual Lorentzian components (thin lines) obtained during deconvolution. Note the major increase of the Lorentzian at 1675 cm^{-1} in the 70 °C-spectrum. Inset to (B) displays the measured spectra at the two different temperatures to aid direct comparison.

of bacterial dUTPase. Fig. 5A indicates that both fluorescence intensity and emission wavelength are convenient indicators to follow unfolding. The process is highly cooperative, in agreement with the data of heat-induced denaturation.

Unfolding of Trp-lacking Drosophila dUTPase cannot be followed by fluorescence spectroscopy because fluorescence of the Drosophila dUTPase Tyr residues did not show any correlation to denaturant concentration, presumably due to the at least partially solvent-exposed character of these residues even in the folded trimer. To circumvent this problem, CD spectroscopy was applied. To decide if this technique generates data comparable to those obtained by fluorescence, Fig. 5B presents parallel measurements on bacterial dUTPase followed by both of these methods. The $D_{50\%}$ values are in perfect agreement, but the unfolding transition followed by CD seems to be less cooperative (Table 3). This difference most probably reflects that

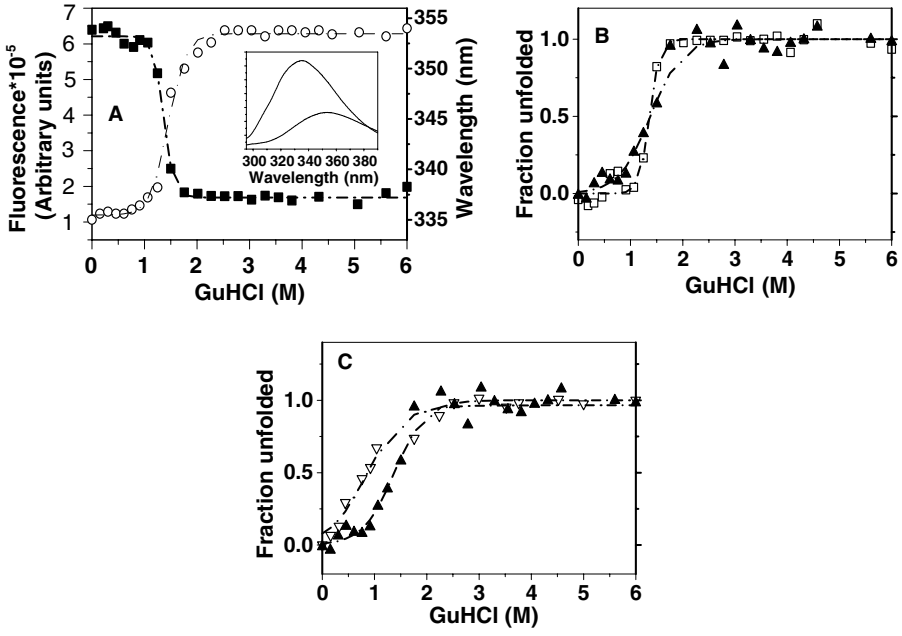

Fig. 5. GuHCl-induced unfolding of bacterial and fruitfly dUTPases. (A, Main) Tryptophan fluorescence intensity at 335 nm (■) and maximum emission wavelength (○) of bacterial dUTPase, excited at 275 nm. Raw data sets were fitted to two-state models according to Eq. (3). (A, Inset) Fluorescence spectra of native and unfolded bacterial dUTPase. From top to bottom: 0 and 6 M GuHCl. (B) Unfolded protein fraction of bacterial dUTPase from fluorescence intensity at 335 nm (□) and molar ellipticity at 222 nm (▲). (C) Unfolded protein fraction of bacterial (▲) and fruitfly dUTPase (1–159) (▽) monitored by molar ellipticity at 222 nm (▲) or 215 nm (▽).

Table 3
Denaturant *m* and $D_{50\%}$ values of dUTPases

Protein	Method	*m* (cal mol^{-1} M)	$D_{50\%}$ (M)
E. coli dUTPase	Fluorescence intensity	26 781	1.36
E. coli dUTPase	Fluorescence maximum emission wavelength	14 727	1.45
E. coli dUTPase	CD intensity	11 581	1.38
Truncated *D. melanogaster* dUTPase	CD intensity	7295	0.84

several secondary structural elements are already perturbed at lower denaturant concentration. However, the close agreement between the $D_{50\%}$ values excludes the possibility of retention of major folded structure at a state where Trp residues become solvent-exposed, indicating disintegration of the trimer. This result corroborates the absence of folded monomers during unfolding of the oligomer (cf. Fig. 2B). Additional support is provided by gel filtration data, which demonstrated trimer retention at 3 M GuHCl (data not shown).

Fig. 5C shows that secondary structural elements of Drosophila dUTPase are perturbed at the very lowest GuHCl concentration indicating strikingly low stability. The significant decrease in $D_{50\%}$ as compared to the value observed with bacterial dUTPase provides further support to this finding. Together with the thermal unfolding data, these results argue for a largely increased sensitivity of fruitfly dUTPase towards diverse perturbing effects.

3.4. Conclusions

Bacterial and Drosophila dUTPases are characterized with largely different stability. The eukaryotic enzyme is significantly less resistant to structural perturbations, let they be induced either by heat or denaturing solvent. Similar low stability was observed in the case of human dUTPase (manuscript in preparation). The increased polarity of the central threefold channel, which is the main structural difference between bacterial and eukaryotic dUTPases, is suggested to render the latter protein more exposed to environmental effects. This increased sensitivity to the environment is reflected not only in decreased stability, but also in ligand induced conformational changes [15], as well as in cooperativity of nucleotide binding [6,7]. It seems that increased sensitivity towards cognate ligands, presumably required in developed organisms, is coupled to some loss of protein stability.

Irrespective of the overall stability, both types of dUTPases were found to unfold in a process where trimer dissociation and monomer unfolding cannot be separated. The scheme in Fig. 2B summarizes these findings to exclude the presence of natively folded monomers. This unfolding pathway underlines the importance of trimeric organization in dUTPases to maintain enzymatic activity.

Acknowledgements: This work was supported by grants of the Hungarian National Research Foundation (OTKA Grant Nos. T 034120, TS 044730, M 27852 to B.G.V.), the Howard Hughes Medical Institutes, USA (Grant No. #55000342 to Research Scholar B.G.V.), the Alexander von Humboldt Foundation, Germany, and the Aventis/Institut de France Scientia Europeae Prize, France (to B.G.V.). We thank István Hajdú for expert help with the FT-IR experiments.

References

[1] Shlomai, J. and Kornberg, A. (1978) J. Biol. Chem. 253, 3305–33012.
[2] Goulian, M., Bleile, B.M., Dickey, L.M., Grafstrom, R.H., Ingraham, H.A., Neynaber, S.A., Peterson, M.S. and Tseng, B.Y. (1986) Adv. Exp. Med. Biol. 195 (Pt B), 89–95.
[3] Larsson, G., Svensson, L.A. and Nyman, P.O. (1996) Nat. Struct. Biol. 3, 532–538.
[4] Gonzalez, A., Larsson, G., Persson, R. and Cedergren-Zeppezauer, E. (2001) Acta Crystallogr. D: Biol. Crystallogr. 57, 767–774.
[5] Fiser, A. and Vertessy, B.G. (2000) Biochem. Biophys. Res. Commun. 279, 534–542.
[6] Dubrovay, Z., Gàspári, Z., Hunyadi-Gulyás, É., Medzihradszky, F.K., Perczel, A. and Vértessy, B.G. (2004) J. Biol. Chem. 279, 17945–17950.
[7] Kovári, J. et al. (2004) J. Biol. Chem. 279, 17932–17944.
[8] Persson, R., Nord, J., Roth, R. and Nyman, P.O. (2002) Prep. Biochem. Biotechnol. 32, 157–172.
[9] Vertessy, B.G., Persson, R., Rosengren, A.M., Zeppezauer, M. and Nyman, P.O. (1996) Biochem. Biophys. Res. Commun. 219, 294–300.
[10] Vertessy, B.G. (1997) Proteins 28, 568–579.
[11] Privalov, P.L. and Potekhin, S.A. (1986) Methods Enzymol. 131, 4–51.
[12] Larsson, G., Nyman, P.O. and Kvassman, J.O. (1996) J. Biol. Chem. 271, 24010–24016.
[13] Vertessy, B.G., Larsson, G., Persson, T., Bergman, A.C., Persson, R. and Nyman, P.O. (1998) FEBS Lett. 421, 83–88.
[14] Nord, J., Nyman, P., Larsson, G. and Drakenberg, T. (2001) FEBS Lett. 492, 228–232.
[15] Kovári, J., Imre, T., Szabó, P. and Vértessy, B.G. (2004) Nucleosides, Nucleotides Nucleic Acids (in press).
[16] Cantor, C.R. and Schimmel, P.R. (1980) W.H. Freeman and Company, San Francisco.
[17] Greenfield, N.J. (1996) Anal. Biochem. 235, 1–10.
[18] Poklar, N., Petrovcic, N., Oblak, M. and Vesnaver, G. (1999) Protein Sci. 8, 832–840.
[19] Privalov, P.L. and Makhatadze, G.I. (1992) J. Mol. Biol. 224, 715–723.
[20] Susi, H. and Byler, D.M. (1986) Methods Enzymol. 130, 290–311.
[21] Prasad, G.S., Stura, E.A., Elder, J.H. and Stout, C.D. (2000) Acta Crystallogr. D: Biol. Crystallogr. 56, 1100–1109.